



SCIENTIFIC REPORTS



OPEN

Articular cartilage and meniscus reveal higher friction in swing phase than in stance phase under dynamic gait conditions

Daniela Warnecke¹ , Maxi Meßmer¹, Luisa de Roy¹, Svenja Stein¹, Cristina Gentilini², Robert Walker², Nick Skaer², Anita Ignatius¹ & Lutz Dürselen¹ 

Most previous studies investigated the remarkably low and complex friction properties of meniscus and cartilage under constant loading and motion conditions. However, both load and relative velocity within the knee joint vary considerably during physiological activities. Hence, the question arises how friction of both tissues is affected by physiological testing conditions occurring during gait. As friction properties are of major importance for meniscal replacement devices, the influence of these simulated physiological testing conditions was additionally tested for a potential meniscal implant biomaterial. Using a dynamic friction testing device, three different friction tests were conducted to investigate the influence of either just varying the motion conditions or the normal load and also to replicate the physiological gait conditions. It could be shown for the first time that the friction coefficient during swing phase was statistically higher than during stance phase when varying both loading and motion conditions according to the physiological gait pattern. Further, the friction properties of the exemplary biomaterial were also higher, when tested under dynamic gait parameters compared to static conditions, which may suggest that static conditions can underestimate the friction coefficient rather than reflecting the *in vivo* performance.

The fibro-cartilaginous menisci play a decisive role within the knee joint. Due to its semi-lunar shape and wedge-shape cross section, it increases the contact area between the incongruent articulating surfaces of femur and tibia, thereby homogenising the load distribution within the joint¹⁻⁴. Additionally, it is involved in joint stabilisation, nutrient distribution and lubrication^{1-3,5,6}. Due to the high loads up to 3 times bodyweight (BW)^{7,8}, which are transmitted through the menisci, it is prone to injuries. Here, the gold standard therapy is still a (partial) meniscectomy, although it has been shown that this can lead to cartilage degeneration in the long-term due to both an increase in contact pressure and a greater friction⁹⁻¹³. Consequently, there is an increased need for treatment strategies to restore and/or replace the meniscus. Among different research approaches, it is not yet possible to replace meniscal tissue by a material that exhibits both satisfying mechanical and tribological performance¹⁴⁻¹⁶. Here, it is stated in the literature that the tribological properties should mimic that of the native tissue as close as possible, thereby friction coefficients less than 0.05 are desirable for a well-functioning replacement material¹⁷. We recently reported friction coefficients of around 0.056 of a silk fibroin scaffold for partial meniscal replacement, which is in the range of the requirements for meniscal replacements postulated by Rongen *et al.*^{17,18}.

The knee as a synovial/diarthrodial joint is a complex biological and mechanical system, which allows articulation and movement over millions of load cycles during a lifespan of more than 80 years¹⁹. This is granted by unique lubrication mechanisms provided by articular cartilage, menisci and synovial fluid and their special biphasic ultrastructure^{1,3,4,20-23}. In general, meniscus and cartilage consist of a fluid (water; 70–85%) and a solid phase, which is composed of a highly specialized extracellular matrix in each of these tissues¹. Both native forms of the tissues exhibit remarkably low friction coefficients of partly less than 0.01^{12,18,23,24}, which are, however, complex as they depend on a variety of parameters, like a variation over time, lubricant, sliding velocity, applied normal load and opposing surface^{19,25-27}. Nevertheless, most previous studies investigated cartilage and

¹Institute of Orthopaedic Research and Biomechanics, Centre for Trauma Research Ulm, Ulm University Medical Centre, Ulm, Germany. ²Orthox Ltd., Abingdon, UK. Correspondence and requests for materials should be addressed to D.W. (email: daniela.warnecke@uni-ulm.de)

meniscus friction under constant normal loading conditions and sliding velocities ranging from 0.02–4 MPa and 0.1–50 mm/s, respectively^{18,23,25,26,28,29}. Based on these static testing conditions and on the three lubrication modes (boundary-, mixed- and fluid lubrication), tribological theories were postulated to describe the low friction properties^{19,28–33}. But taking into account that during gait the tibiofemoral contact loads acting parallel to the tibial axis (axial load)³⁴ as well as the velocity of femoral and tibial surfaces relative to each other vary considerably^{35–37}, it is obvious that the testing conditions used so far do not reflect the conditions typically occurring *in vivo*^{18,19,28–33}. In general, a gait cycle of one leg can be divided into a stance phase (60%) initiated by heel strike and terminated by toe-off and a swing phase (40%), respectively. The tibiofemoral contact forces differ considerably between both phases. While a double-peak loading characteristic of 2–3 times BW occur within stance phase, the loads during swing phase are much lower^{34,38,39}. Simultaneously, the surfaces of femur, meniscus and tibia move relative to each other. During stance phase the knee flexion angle increases from 0° at heel strike to a maximum of 15°, while during swing phase the flexion angle rises to approximately 60°^{34–38}. This results in relative velocities between the articulating surfaces of 150 mm/s in average during stance- and up to 300 mm/s during swing phase^{19,35}, which is far beyond the velocities that were typically used in previous friction studies. To the best of our knowledge, there are only two studies assessing the friction of the physiologically articulating surfaces and a meniscal replacement material under sinusoidal²⁷ or simulated physiological loading conditions of the knee joint, respectively¹⁶. However, both used constant sliding velocities of 1 mm/s²⁷ and 4 mm/s¹⁶, which were not in the range of physiological velocities in the knee joint^{35,36}. Consequently, there is a lack of information in literature regarding the influence of both continuously varying the sliding velocity and simultaneously varying loading and motion conditions according to a gait cycle on friction coefficient of articular surfaces. Thus, the aim of this study was first to investigate the friction properties of the articulating surfaces within the knee joint – meniscus and articular cartilage – under testing conditions characteristically occurring within the joint during walking and second, to examine the influence of these simulated physiological testing conditions also on a potential biomaterial for meniscal replacement and therefore making possible predictions regarding its chondroprotective effect *in vivo*. Therefore, a dynamic friction testing device was developed in a *pin-on-plate* testing configuration applying normal, gait-related loading and motion conditions derived from stance- and swing phase to material pairings of articular cartilage, meniscus and a silk fibroin based hydrogel scaffold. To quantify the friction properties, the friction coefficient μ was identified throughout the tests.

Material and Methods

Sample preparation. Ten fresh bovine knee joints were ordered from a local butcher and frozen at -20°C until the day before testing. After thawing for 1 day at 4°C , the knees joints were examined in terms of integrity and dissected according to our standard protocol. Cylindrical meniscus and cartilage as well as the flat cartilage samples were harvested out of each knee joint as previously described within the static friction study of the silk fibroin scaffold using a trephine drill or a biopsy punch ($\varnothing = 6\text{ mm}$) and a peeler, respectively¹⁸. As an additional testing material, ten cylindrical samples were punched out of flat sheets (initial height: $4.9 \pm 0.2\text{ mm}$) of material for meniscal replacement (FibroFix Meniscus, Orthox Ltd.) using a 6 mm biopsy punch, as well.

Dynamic friction testing device. To investigate the frictional behaviour of the different material pairings under physiological testing conditions, a dynamic materials testing machine (ElectroForce 5500, including a 1 DOF load cell, 200 N, accuracy class $\leq 1\%$, WMC-50-456, both BOSE/TA Instruments, New Castle, USA) was equipped with a linear motor (linear stage VT-75, PI miCos GmbH, Eschbach, Germany) mounted on a customized aluminium frame (Fig. 1). The aluminium frame comprised four linear guidances, an intermediate plate, a ball cushion, a *pin* sample holder and a second load cell for measuring the resultant friction force F_F (3 DOF, maximum $F_{x,y} = 20\text{ N}$, maximum $F_z = 50\text{ N}$; accuracy class: 0.5%; ME-Meßsysteme GmbH, Henningsdorf, Germany). Additional counter weights were installed to prevent any load application to the *pin* due to the tare weight of the frame. The linear motor, carrying the flat cartilage sample within a sample well, moved the *plate* sample holder in reciprocating manner.

Next to quasi-static testing conditions, the dynamic materials testing machine provided dynamic, freely configurable load application profiles to the *pin*. Using this feature, it was possible to generate loading conditions acting in the knee joint during normal level walking at a physiological walking speed of 5 km/h. Hence, a double-peak loading regime was applied representing the stance phase ($p_{max,1} \cong 0.9\text{ MPa}$, $p_{max,2} \cong 0.8\text{ MPa}$) followed by a low load plateau ($p \cong 0.2\text{ MPa}$) simulating the swing phase in the knee joint³⁴. Simultaneously, the stage motor, driven in a position controlled mode, followed up the distances that were ran over during both phases of a gait cycle in a defined period of time of 1.1 s. The input data were defined by assuming a constant radius of the femoral condyles of $r = 25\text{ mm}$ as well as 15° and 60° as the maximum flexion angles during stance and swing phase, respectively. The resultant stroke lengths of 6 mm for stance- and 25 mm for swing phase were calculated using the radian measure (1).

$$b = \pi r \frac{\alpha}{180} \quad (1)$$

To ensure that both actuators, the linear motor and dynamic materials testing machine, were moving synchronously, every simulated gait cycle a trigger signal was sent by the dynamic materials testing machine to a custom-made LabVIEW program (LabVIEW, National Instruments, Austin, USA). This software was developed to control the linear motor and processes these signals for data acquisition, whereby the applied normal force F_N and the resultant friction force F_F were continuously recorded (sample rate: 100 Hz) to determine the friction coefficient μ (2).

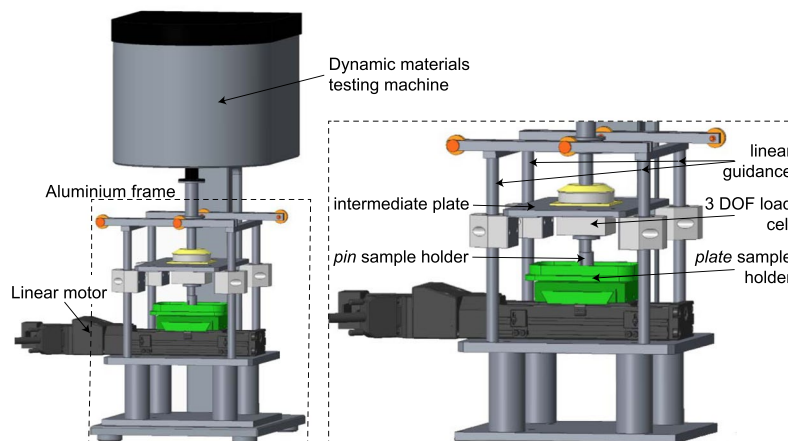


Figure 1. Dynamic friction testing device consisting of a dynamic materials testing machine (ElectroForce 5500, including a 1 DOF load cell, 200 N, accuracy class $\leq 1\%$, WMC-50-456, both BOSE/TA Instruments, New Castle, USA) equipped with a linear motor (linear stage VT-75, PI miCos GmbH, Eschbach, Germany), which was mounted on an additional aluminium frame (left). This frame was designed out of four linear guidance, an intermediate plate, a ball cushion (not shown in detail), the pin sample holder, a second load cell for measuring the resultant friction force F_F (3 DOF, maximum $F_{x,y} = 20$ N, maximum $F_z = 50$ N; accuracy class: 0.5%; ME Meßsysteme GmbH, Henningsdorf, Germany) (right) and additional counter weights (not shown).

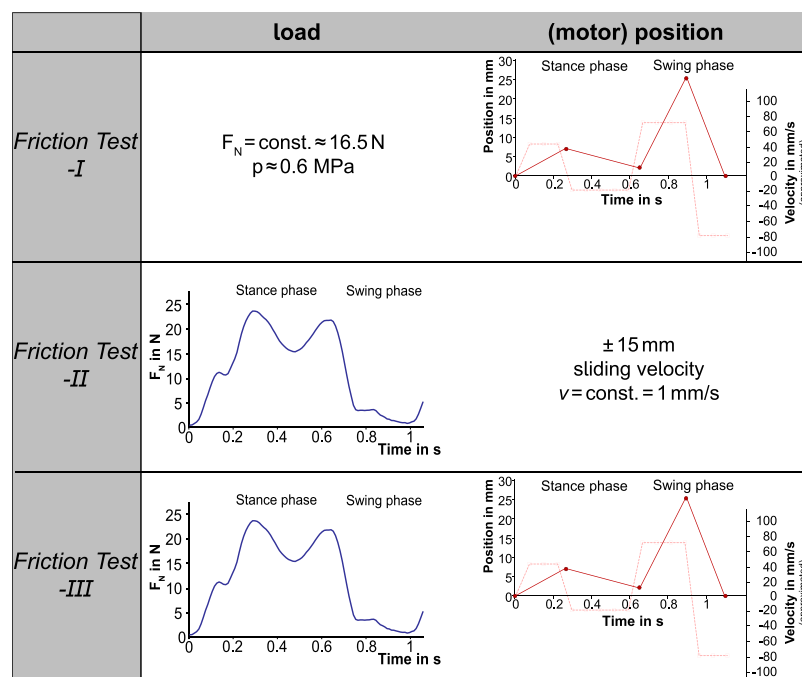


Figure 2. Overview of the three friction test scenarios and the resultant applications of load (F_N) and motion: (motor) position and the approximated velocity in mm/s.

$$\mu = \frac{F_F}{F_N} \tag{2}$$

Testing protocol. As the current study is the first synchronously applying loading and motion conditions typically occurring in the knee joint during stance- and swing phase to the mentioned friction pairings, the influence of just varying normal load F_N or velocity v on their friction properties should be additionally addressed. Therefore, the testing protocol was divided into three test scenarios (FT-I, -II, -III) conducted on three consecutive days (Fig. 2).

Based on the literature showing a decrease in the friction coefficient of articular cartilage when the testing velocity exceeds 50 mm/s^{14,26}, on the first experimental day, each cylindrical sample (meniscus M, tibial cartilage TC and FibroFix Meniscus scaffold S) was tested against the corresponding flat femoral cartilage sample (FC) under constant axial loading conditions ($p = 0.5\text{--}0.6$ MPa, acc. to¹⁸) and varying velocities according to stance- and swing phase of a human gait cycle with a physiological walking speed of 5 km/h (Fig. 2: FT-I).

To validate the dynamic friction testing device with the literature especially with the two studies investigating cartilage and/or meniscus friction as well as the friction properties of a potential material for meniscal replacement^{16,27}, a second friction test (FT-II) was added to the testing protocol. Here, the sliding velocity of the *plate* was kept constant (1 mm/s) as previously done¹⁸ and the load application to the *pin* (F_N) varied cyclically according to the double-peak loading regime acting during stance phase followed by a low plateau simulating the swing phase of a gait cycle (Fig. 2: FT-II).

The third friction test (FT-III) combined both dynamic load and motion application to test the material pairings under conditions best resembling normal gait (Fig. 2: FT-III).

This resulted in a total of three tests per friction pairing (e.g. TC1/M1/S1 vs. FC1) each with a testing duration set to 20 minutes. Throughout the whole testing period, special attention was paid that all samples had the same recovery time without any load application once between each test within a test scenario (FT-I, -II, -III) but also between the test scenarios themselves (>12 h in PBS at 4 °C). The tests were performed at room temperature of approximately 24 °C and a humidity of approximately 21%. Ovine synovial fluid aspirated from skeletally healthy knee joints directly after slaughtering, served as a lubricant. Throughout the testing period, care was taken that the samples were fully covered with lubricant.

Statistics. The friction coefficient μ ($\mu = F_f/F_N$) was determined at the onset (μ_0) and at the end of the testing duration of 20 minutes (μ_{end}) using a customized MATLAB script. (MATLAB R2013b, The MathWorks Inc., Natick, USA.). Therefore, μ of the first and last three simulated gait cycles were averaged for μ_0 and μ_{end} , respectively, each additionally separated for stance- and swing phase.

Based on the previous static friction study¹⁸, a power analysis was performed to detect differences in the friction coefficient between the friction pairings (M, TC, S vs. FC) using G*Power⁴⁰. A total sample size of 5 was calculated to get an actual power of 0.99. Due to the complexity of the defined testing protocol, the maximum calculated samples size was doubled leading to a final total samples size of $n = 10$.

All further statistical analyses were performed using GraphPad Prism[®] software (GraphPad Software Inc., La Jolla, USA).

1. The effect of the testing duration on the friction coefficient (here the comparison of μ_0 and μ_{end}) of the different friction pairings (M, TC, S vs. FC) within each specific test scenario (FT-I, -II, -III), were evaluated using repeated measures one-way Analyses of Variances (ANOVA) with Sidak's post hoc test for multiple comparison, if the data were normally distributed. Otherwise, the nonparametric Friedman test with Dunn's post hoc test for multiple comparison were conducted.
2. To determine differences in the friction coefficient of stance- and swing phase due to the different load patterns in the test scenarios (FT-I vs. FT-II vs. FT-III) for each friction pairing (M, TC, S vs. FC), one-way ANOVAs with Sidak's post hoc test for multiple comparison were performed, if the data were normally distributed. Otherwise, the nonparametric Friedman test with Dunn's post hoc test for multiple comparison were conducted.
3. To compare the friction coefficients of stance- and swing phase between the friction pairings (M, TC, S vs. FC) for each test scenario (FT-I, -II, -III), mixed-effects analysis (REML) with Tukey's post hoc test for multiple comparison were accomplished.

The statistical significance level was set to $p < 0.05$.

Results

A summary of all friction coefficients (μ_0 and μ_{end}) obtained during the three test scenarios (FT-I, -II, -III) separated for both phases of a gait cycle, stance- and swing phase as well as for the friction pairings: tibial cartilage (TC), meniscus (M) and the silk fibroin scaffold (S) each against a flat, femoral cartilage sample (FC) are given in Table 1 as mean \pm standard deviation (SD). Here, the three different test scenarios were established to determine the influence of only varying the sliding velocity (FT-I) or normal force F_N (FT-II) according to the motion and loading conditions during gait, and finally the combination of both as the most physiological friction test (FT-III).

The evaluation of the friction coefficient revealed no time-dependent differences (μ_0 vs. μ_{end}) for each material pairing (M, TC or S vs. FC). This was also true for each of the three test scenarios (FT-I, -II, -III; Fig. 3). Consequently, all other analyses and comparisons were performed using the friction coefficient determined after 20 minutes testing (μ_{end}).

No differences between the friction coefficients obtained during simulated stance- and swing phase could be found for both cartilaginous tissues, meniscus and tibial cartilage, each tested against flat cartilage samples when varying only the velocity (FT-I) or normal load (FT-II). Interestingly, this changed as soon as both testing parameters synchronously varied as it occurs during a physiological gait cycle (FT-III). Here, the simulated low-loaded swing phase revealed significantly higher friction coefficients than the stance phase (Fig. 3, left and central column). Additionally, the friction coefficient of meniscus against cartilage (M vs. FC) was highest for FT-III (0.030 ± 0.008) during swing phase in comparison to the other two load scenarios (FT-I and -II, 0.017 ± 0.006 and 0.017 ± 0.012 , respectively), while during stance phase no differences in friction could be found for each of the three different test scenarios ($p \leq 0.05$; Fig. 4b). However, the cartilage against cartilage pairing remained in general uninfluenced by the different load scenarios for both, stance- and swing phase (Fig. 4a). The silk fibroin

FT-I	TC vs. FC		M vs. FC		S vs. FC	
	Stance- &	swing phase	Stance- &	swing phase	Stance- &	swing phase
μ_0	0.022 ± 0.012	0.025 ± 0.010	0.019 ± 0.008	0.017 ± 0.005	0.034 ± 0.013	0.036 ± 0.014
μ_{end}	0.018 ± 0.005	0.024 ± 0.009	0.020 ± 0.006	0.017 ± 0.006	0.036 ± 0.011	0.038 ± 0.009
FT-II						
μ_0	0.021 ± 0.013	0.027 ± 0.018	0.026 ± 0.024	0.030 ± 0.028	0.077 ± 0.041	0.122 ± 0.058
μ_{end}	0.013 ± 0.010	0.019 ± 0.021	0.015 ± 0.010	0.017 ± 0.012	0.061 ± 0.034	0.092 ± 0.046
FT-III						
μ_0	0.018 ± 0.005	0.032 ± 0.013	0.015 ± 0.009	0.033 ± 0.007	0.042 ± 0.017	0.043 ± 0.021
μ_{end}	0.019 ± 0.005	0.029 ± 0.009	0.016 ± 0.007	0.030 ± 0.008	0.057 ± 0.019	0.047 ± 0.020

Table 1. Summary of all friction coefficients (mean ± standard deviation) obtained during the three different test scenarios: FT-I ($F_N = \text{const.}$, v acc. to gait cycle), -II (F_N acc. to gait cycle, $v = \text{const.}$) and -III (F_N and v acc. to gait cycle) for the friction pairings: tibial cartilage (TC), meniscus (M) and the silk fibroin scaffold (S) each against a flat, femoral cartilage sample (FC).

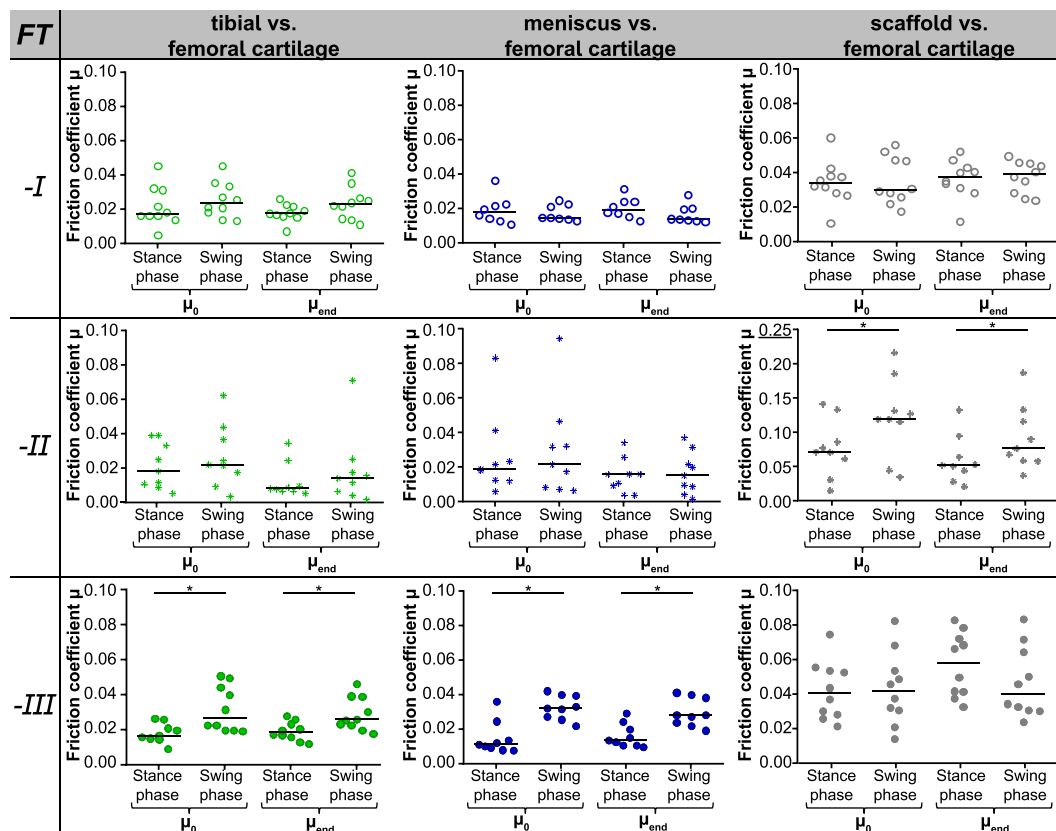


Figure 3. Comparison of the friction coefficients (median with raw data) for each material pairing (M, TC, S vs. FC, divided by column) obtained in the three different friction test scenarios (FT-I: $F_N = \text{const.}$, v acc. to gait cycle, FT-II: F_N acc. to gait cycle, $v = \text{const.}$, FT-III: F_N and v acc. to gait cycle, divided by rows). * $p \leq 0.05$ with a minimum actual power of 70.1% (FT-II scaffold vs. femoral cartilage).

scaffold tested against cartilage showed in general higher friction coefficients under FT-II conditions (averaged stance phase: $\mu = 0.069 \pm 0.011$ and swing phase: $\mu = 0.107 \pm 0.021$; Fig. 3, right column), which was additionally statistically significant in comparison to FT-I and FT-III (0.038 ± 0.009 and 0.047 ± 0.020 , respectively) during swing phase (Fig. 4c).

Testing the material pairings either under constant loads but varying velocities (FT-I) or inversely varying the normal forces F_N according to the loading conditions during normal walking at 5 km/h but maintaining a constant velocity (1 mm/s, FT-II), the silk fibroin scaffold revealed the highest friction coefficients in comparison to tibial cartilage- and meniscus samples, for both, stance- and swing phase, respectively (Fig. 5a,b). This was also true during stance phase when testing under simulated physiological loading and motion conditions (FT-III, Fig. 5c). Even though, the scaffold showed a higher friction coefficient by tendency also during swing phase, no

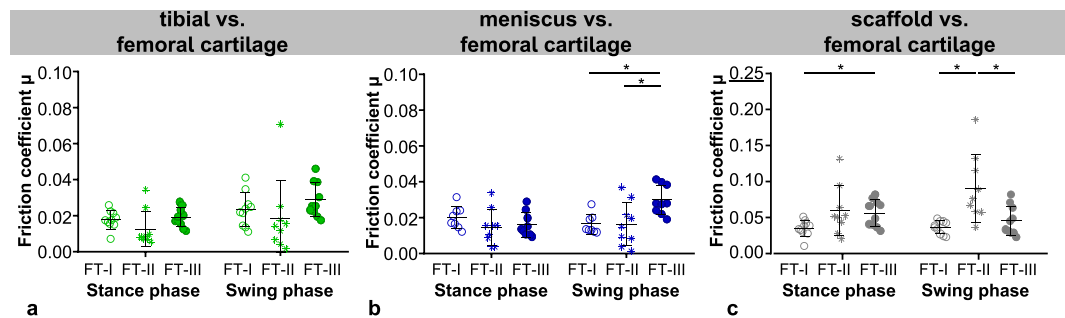


Figure 4. Comparison of the friction coefficients (μ_{end}) obtained for each material pairing: tibial cartilage (a), meniscus (b) and scaffold (c) each against femoral cartilage within the three different friction test scenarios ($n = 8-10$, mean \pm standard deviation and raw data; \circ FT-I, \ast FT-II, \bullet FT-III), $\ast p \leq 0.05$ with a minimum actual power of 96.1% and 73.1% for the comparisons the meniscus and scaffold friction coefficient, respectively.

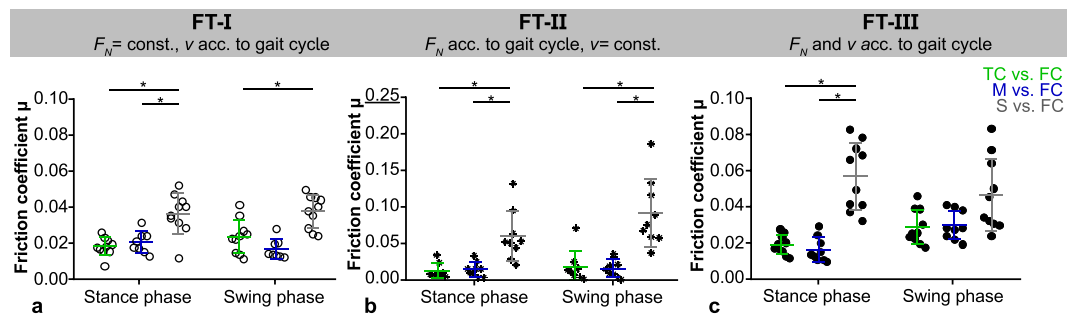


Figure 5. Comparison of the friction coefficients (μ_{end}) obtained within each friction test scenarios (\circ FT-I: A, \ast FT-II: B, \bullet FT-III: C) for the different material pairings (TC, M, S vs. FC; $n = 8-10$, mean \pm standard deviation and raw data) $\ast p \leq 0.05$ with an actual power of approximately 99%.

statistical differences were detected. The friction coefficient of meniscus and tibial cartilage each against femoral cartilage did not differ statistically during all three test scenarios.

Discussion

For the first time we were able to assess friction coefficients of the articulating surfaces of the knee joint, meniscus and articular cartilage, under simulated physiological loading and motion conditions occurring during normal walking. Additionally, a silk fibroin scaffold was used for testing to investigate the influence of these new testing conditions on a potential material for meniscal replacement.

When tested under physiological testing conditions (FT-III), the friction coefficients for both cartilaginous tissues, tibial cartilage and meniscus, each tested against cartilage (TC/M vs. FC) were higher during the low-loaded swing phase (TC vs. FC: 0.029 ± 0.009 , M vs. FC: 0.030 ± 0.008) than during the high-loaded stance phase (TC vs. FC: 0.019 ± 0.005 , M vs. FC: 0.016 ± 0.007). Although this phenomenon appears contradictory, Majd *et al.* and Krishnan *et al.* showed an increase in friction within low-loaded phases, as well^{16,27}. Krishnan *et al.* simultaneously detected negative values of the fluid load support W^P/W of less than -1.75 ²⁷ and consequently made the assumption that suction might occur between the cartilage and the counter glass platens^{16,27}. This additionally led to an increased solid-to-solid contact force, resulting in higher friction coefficient, although the applied normal force is smallest²⁷. Thus, once the load is rapidly decreased, the contact between the loaded cartilage-*pin* and glass after a long load application might lead to a sticking of the cartilage to the glass *plate*. Even if in both studies (inter alia) an impermeable opposing surface (e.g. glass) was used^{16,27}, this phenomenon could also be observed with flat cartilage samples as counterpart during the current study especially in FT-III (and FT-II for S vs. FC), when dynamically varying the axial load. Despite the fact that Krishnan *et al.* and Majd *et al.* applied a constant velocity of 1 mm/s and 4 mm/s^{16,27}, respectively, which is far below the surface velocities in the knee joint of 50–300 mm/s³⁵, their testing conditions compared well with our second friction test (FT-II) also carried out at 1 mm/s. Here, the silk fibroin scaffold generally showed the highest friction coefficients, which were again significantly increased within the low-loaded swing phase (0.092 ± 0.046 ; stance phase: 0.061 ± 0.034). This is again in line with the study of Majd *et al.* evaluating the friction properties of another potential material for meniscal repair under similar conditions. These authors found a more than 15-fold higher friction coefficient of the replacement material during swing phase than during stance phase (approximately 0.7 vs 0.04), while during swing phase μ of the silk fibroin based hydrogel scaffold tested in the current study was only 50% higher¹⁶. In consideration of the different lubricants used of Majd *et al.* and the current study (solution of PBS and different lubrication molecules vs. synovial fluid, respectively), the obtained results fit nevertheless quite well to the results of the referenced study (stance phase: 0.06 vs 0.04), which showed the validity of the testing device.

Next to the soaking effect and the resultant rise in the friction coefficient when the applied force rapidly decreases at the transition of stance- and swing phase, it is also known that a quite thick fluid film of approximately 1.6 μm can be formed during swing phase^{19,35} that is much larger than the average surface roughness of articular cartilage ($R_a = 200 \text{ nm}$). Transferring these to the simulated gait conditions (FT-III) of the current study, it can be concluded that together with the assumed high Hersey number (low normal load and high velocity), hydrodynamic lubrication occurs in the swing phase^{19,26}. This fluid film is subsequently squeezed out due to the rapid increase in load at ‘heel strike’ with beginning of the stance phase. Since, this load application has an impact characteristic ($<0.1 \text{ s}$), the fluid film is pressurised but can be preserved between the deformable bearing material of meniscus and/or cartilage. Taking the identified low friction coefficient in the upcoming stance phase of <0.02 into account, elasto-hydrodynamic lubrication can be assumed as this is the lubrication mode of least friction coefficient in the Stribeck curve¹⁹. Throughout a stance phase of low velocity-to-load ratio, the synovial fluid still separates the articulating surfaces until ‘toe off’ and the initiation of the next swing phase. The distinct lubrication mechanisms of elasto-hydrodynamic- and hydrodynamic lubrication within the simulated stance- and swing phase can consequently be an explanation for the obtained differences in the friction coefficients between these gait phases when testing under physiological loading and motion conditions (FT-III). However, tibial cartilage samples were rather uninfluenced by the three different loading scenarios. The cartilage – cartilage friction pairing indeed showed by tendency the lowest friction coefficient of approx. $\mu = 0.013$ during stance- and $\mu = 0.019$ during swing phase and when testing under varying loading (FT-II) conditions, while μ was nearly identical during FT-I and FT-III (stance phase: $p = 0.6415$, swing phase: $p = 0.3163$). This indicates that additionally varying the velocity in a physiological range affect cartilage friction. The authors speculate that a reason might be the differences in the extracellular matrix (ECM) compositions of articular cartilage and meniscal tissue. Since with progressive duration of friction testing, the interstitial fluid of the loaded cylindrical samples (*pin*) of both tissues is squeezed out, the applied load is carried by their ECM and is therefore responsible for the friction coefficient. While the ECM of articular cartilage is composed of 5–10% wet wt. of proteoglycans (PG), meniscal tissue contains only a fifth of this¹. Additionally, their main collagen type differ, as well: articular cartilage: 10–20% wet wt. collagen type II vs. meniscal tissue: 15–25% wet wt. collagen type I, which may alter the resistance to high velocities and consequently shear forces of the tissue^{1–4}.

It was already shown that the friction coefficients of meniscus and cartilage are multifactorial depending on several parameters and operating conditions²⁶ rather than being just a material constant as described within Coulomb’s friction law. Consequently, the mechanisms of the mentioned lubrication modes will significantly differ depending on the testing parameters, as well^{26,41}. Although, it is important to perform friction tests under clearly defined static testing and lubrication regimes²⁶, one should be aware that such data do not perfectly reflect the friction coefficients occurring *in vivo*, e.g. during gait. This is supported by the literature as there is a general consent that (elasto-)hydrodynamic- but also mixed lubrication mechanisms can synergistically contribute to the remarkably low friction properties of the joint^{19,42} as the loading and motion conditions vary considerably within a normal gait cycle.

As a potential material for meniscal replacement, a silk fibroin based hydrogel scaffold was additionally tested under the three different testing conditions (FT-I, -II and -III). In a previous study, the scaffold already showed friction coefficients of 0.056, which was higher than friction of native meniscus ($\mu = 0.021$) but in the range of the requirements for meniscal replacement postulated by Rongen *et al.*¹⁷. Within the current study the material met these requirements again also under simulated gait conditions (FT-III: 0.057 ± 0.019 and 0.047 ± 0.020 for stance and swing phase, respectively).

Since the physiological testing conditions revealed higher friction coefficients for meniscal tissue especially within the simulated swing phase of almost 0.030, this suggests that static testing methods as reported in the literature with friction coefficients of less than 0.01 can underestimate friction coefficients rather than reflecting the complex *in vivo* performance. This might especially be important for potential replacement materials and their prediction regarding their chondroprotective effect *in vivo*.

For all three tests (FT-I, -II, -III) in general, no time-dependent differences in the friction coefficient (μ_0 vs. μ_{end}) could be observed for each material pairing (M, TC or S vs. FC) either during stance- or during swing phase. However, this was not surprising as previous studies already showed that if the moving opposing surface (*plate*) is cartilaginous, no increase in friction will develop^{18,23,43}. Consequently, the interstitial fluid pressurization was maintained in all three test scenarios as well as for all material pairings. While the *pin* was loaded throughout the whole test, the moving contact area of the flat cartilage surface (*plate*) was able to recover during the time of unloading before it was loaded again. Therefore its fluid phase supported the load during the whole testing duration and thus, the friction coefficient remained at the observed low level.

Limitations. The friction testing device developed in the current study was designed according to a *pin-on-plate* configuration. Using this test setup, it was possible to apply loads and velocities occurring in the knee joint during normal walking. However, it is a simplification of the complex joint kinematics as the combined rolling and sliding motion coexisting during flexion and extension of the knee joint is not considered. Nevertheless, using a “rolling-gliding wear simulator” it was already shown that during rolling, and rolling with slip motion, the signs of wear were least when testing different artificial material pairings⁴⁴. Consequently, the main part of friction occurs during sliding, which was considered within the dynamic friction testing device investigated in the current study. Nevertheless, to further take the rolling and sliding within the knee joint into account during friction analysis, a pendulum friction simulator would be an alternative test setup. The advantage of this test setup is that the entire knee joint is tested and therefore considered as one biomechanical and tribological system, preserving the physiological geometries and joint kinematics^{45–47}. However, this also represents a disadvantage, since no distinction can be made between friction properties of cartilage and/or meniscus.

Conclusion. The current study presents new insights in joint friction mechanics as it showed significantly lower friction coefficients during simulated stance- than during the low-loaded swing phase. This phenomenon was observed for meniscus and articular cartilage only when testing under conditions with varying both normal load and velocity as it appears during gait. The high velocities occurring in the swing phase may cause a transition from elasto-hydrodynamic to hydrodynamic lubrication and therefore, increased friction coefficient. Consequently, due to the multifactorial characteristics of cartilage and meniscus friction, the current study emphasizes the need of adding friction tests under physiological testing conditions to the tribological characterisation of materials relevant for joints and especially for potential meniscal or cartilage replacement materials. Thereby, the tested silk fibroin based hydrogel scaffold matched the friction coefficient as demanded in the basic requirements for meniscal replacement materials.

References

- Mow, V. C. & Huiskes, R. Structure and function of articular cartilage and meniscus, Third Edition. In: *Basic Orthopaedic Biomechanics & Mechano-Biology* (eds Mow, V. C. & Huiskes, R.), 182–257 (Lippincott Williams & Wilkins, 2005).
- Masouros, S. D., McDermott, I. D., Amis, A. A. & Bull, A. M. Biomechanics of the meniscus-meniscal ligament construct of the knee. *Knee Surg Sports Traumatol Arthrosc.* **16**(12), 1121–32 (2008).
- Masouros, S. D., McDermott, I. D., Bull, A. M. & Amis, A. A. Biomechanics, In: *The Meniscus* (eds Beaufils, P. & Verdonk, P.), 29–37 (Springer, 2010).
- McDermott, I. D., Masouros, S. D., Bull, A. M. & Amis, A. A. Anatomy, In: *The Meniscus* (eds Beaufils, P. & Verdonk, R.), 11–18 (Springer, 2010).
- Bullough, P. G., Munuera, L., Murphy, J. & Weinstein, A. M. The strength of the menisci of the knee as it relates to their fine structure. *J Bone Joint Surg Br.* **52**(3), 564–7 (1970).
- Brindle, T., Nyland, J. & Johnson, D. L. The meniscus: review of basic principles with application to surgery and rehabilitation. *J Athl Train.* **36**(2), 160–9 (2001).
- Kutzner, I. *et al.* Loading of the knee joint during activities of daily living measured *in vivo* in five subjects. *J Biomech.* **43**(11), 2164–73 (2010).
- Pena, E., Calvo, B., Martinez, M. A., Palanca, D. & Doblare, M. Finite element analysis of the effect of meniscal tears and meniscectomies on human knee biomechanics. *Clin Biomech.* **20**(5), 498–507 (2005).
- Fairbank, T. J. Knee joint changes after meniscectomy. *J Bone Joint Surg Br.* **30B**(4), 664–70 (1948).
- Fukubayashi, T. & Kurosawa, H. The contact area and pressure distribution pattern of the knee. A study of normal and osteoarthrotic knee joints. *Acta Orthop Scand.* **51**(6), 871–9 (1980).
- Baratz, M. E., Fu, F. H. & Mengato, R. Meniscal tears: The effect of meniscectomy and of repair on intraarticular contact areas and stress in the human knee. A preliminary report. *Am J Sports Med.* **14**(4), 270–5 (1986).
- McCann, L., Ingham, E., Jin, Z. & Fisher, J. Influence of the meniscus on friction and degradation of cartilage in the natural knee joint. *Osteoarthr Cartil.* **17**(8), 995–1000 (2009).
- Seitz, A. M., Lubomierski, A., Friemert, B., Ignatius, A. & Dürselen, L. Effect of partial meniscectomy at the medial posterior horn on tibiofemoral contact mechanics and meniscal hoop strains in human knees. *J Orthop Res.* **30**(6), 934–42 (2012).
- Gleghorn, J. P. *et al.* Analysis of frictional behavior and changes in morphology resulting from cartilage articulation with porous polyurethane foams. *J Orthop Res.* **28**(10), 1292–9 (2010).
- Maher, S. A. *et al.* A pre-clinical test platform for the functional evaluation of scaffolds for musculoskeletal defects: the meniscus. *HSS J.* **7**(2), 157–63 (2011).
- Majd, S. E. *et al.* An *in vitro* study of cartilage-meniscus tribology to understand the changes caused by a meniscus implant. *Colloids Surf B Biointerfaces.* **155**, 294–303 (2017).
- Rongen, J. J., van Tienen, T. G., van Bockhove, B., Grijpma, D. W. & Buma, P. Biomaterials in search of a meniscus substitute. *Biomaterials.* **35**(11), 3527–3540 (2014).
- Warnecke, D. *et al.* Friction properties of a new silk fibroin scaffold for meniscal replacement. *Tribol Int.* **109**, 586–592 (2017).
- Neu, C. P., Komvopoulos, K. & Reddi, A. H. The interface of functional biontribology and regenerative medicine in synovial joints. *Tissue Eng Part B Rev.* **14**(3), 235–47 (2008).
- Mow, V. C., Kuei, S. C., Lai, W. M. & Armstrong, C. G. Biphasic creep and stress relaxation of articular cartilage in compression? Theory and experiments. *J Biomech Eng.* **102**(1), 73–84 (1980).
- Ateshian, G. A. & Wang, H. A theoretical solution for the frictionless rolling contact of cylindrical biphasic articular cartilage layers. *J Biomech.* **28**(11), 1341–55 (1995).
- Soltz, M. A. & Ateshian, G. A. Experimental verification and theoretical prediction of cartilage interstitial fluid pressurization at an impermeable contact interface in confined compression. *J Biomech.* **31**(10), 927–34 (1998).
- Caligaris, M. & Ateshian, G. A. Effects of sustained interstitial fluid pressurization under migrating contact area, and boundary lubrication by synovial fluid, on cartilage friction. *Osteoarthr Cartil.* **16**(10), 1220–7 (2008).
- McCann, L. *et al.* Tribological testing of articular cartilage of the medial compartment of the knee using a friction simulator. *Tribol Int.* **41**(11), 1126–1133 (2008).
- Forster, H. & Fisher, J. The influence of loading time and lubricant on the friction of articular cartilage. *Proc Inst Mech Eng H.* **210**(2), 109–19 (1996).
- Gleghorn, J. P. & Bonassar, L. J. Lubrication mode analysis of articular cartilage using Stribeck surfaces. *J Biomech.* **41**(9), 1910–8 (2008).
- Krishnan, R., Mariner, E. N. & Ateshian, G. A. Effect of dynamic loading on the frictional response of bovine articular cartilage. *J Biomech.* **38**(8), 1665–73 (2005).
- McCutchen, C. W. The frictional properties of animal joints. *Wear.* **5**, 1–17 (1962).
- Walker, P. S., Dowson, D., Longfield, M. D. & Wright, V. “Boosted lubrication” in synovial joints by fluid entrapment and enrichment. *Ann Rheum Dis.* **27**(6), 512–20 (1968).
- Ateshian, G. A. & Mow, V. C. Friction, lubrication, and wear of articular cartilage and diarthrodial joints, Third Edition. In: *Basic Orthopaedic Biomechanics & Mechano-Biology* (eds Mow, V. C. & Huiskes, R.), 447–493 (Lippincott Williams & Wilkins, 2005).
- Jahn, S., Seror, J. & Klein, J. Lubrication of Articular Cartilage. *Annu Rev Biomed Eng.* **18**, 235–58 (2016).
- Medley, J. B., Dowson, D. & Wright, V. Transient elasto-hydrodynamic lubrication models for the human ankle joint. *Eng Med.* **13**(3), 137–51 (1984).
- Hou, J. S., Mow, V. C., Lai, W. M. & Holmes, M. H. An analysis of the squeeze-film lubrication mechanism for articular cartilage. *J Biomech.* **25**(3), 247–59 (1992).
- ISO, B., 14243-1, Implants for surgery–Wear of total knee joint prostheses– Part 1: Loading and displacement parameters for wear-testing machines with load control and corresponding environmental conditions for test (2009).
- Unsworth, A. Tribology of human and artificial joints. *Proc Inst Mech Eng H.* **205**(3), 163–72 (1991).
- Andriacchi, T. P., Dyrby, C. O. & Johnson, T. S. The use of functional analysis in evaluating knee kinematics. *Clin Orthop Relat Res.* **410**, 44–53 (2003).

37. Andriacchi, T. P., Johnson, T. S., Hurwitz, D. E. & Natarajan, R. N. Musculoskeletal Dynamics, Locomotion, and Clinical Applications, Third Edition. In: *Basic Orthopaedic Biomechanics & Mechano-Biology* (eds Mow, V. C. & Huiskes, R.), 91–121 (Lippincott Williams & Wilkins, 2005).
38. Taylor, W. R., Heller, M. O., Bergmann, G. & Duda, G. N. Tibio-femoral loading during human gait and stair climbing. *J Orthop Res.* **22**(3), 625–32 (2004).
39. Heinlein, B. *et al.* ESB Clinical Biomechanics Award 2008: Complete data of total knee replacement loading for level walking and stair climbing measured *in vivo* with a follow-up of 6–10 months. *Clin Biomech (Bristol, Avon)*. **24**(4), 315–26 (2009).
40. Faul, F., Erdfelder, E., Lang, A. G. & Buchner, A. G*Power 3: a flexible statistical power analysis program for the social, behavioral, and biomedical sciences. *Behav Res Methods*. **39**(2), 175–91 (2007).
41. Hersey, M. D. The laws of lubrication of horizontal journal bearings. *J Wash Acad Sci.* **4**(19), 542–552 (1914).
42. Thier, S. & Tonak, M. Influence of Synovial Fluid on Lubrication of Articular Cartilage *in Vitro*. *Z Orthop Unfallchir.* **156**(2), 205–213 (2018).
43. Shi, L., Sikavitsas, V. I. & Striolo, A. Experimental friction coefficients for bovine cartilage measured with a pin-on-disk tribometer: testing configuration and lubricant effects. *Ann Biomed Eng.* **39**(1), 132–46 (2011).
44. Richter, B. I., Ostermeier, S., Turger, A., Denkena, B. & Hurschler, C. A rolling-gliding wear simulator for the investigation of tribological material pairings for application in total knee arthroplasty. *Biomedical engineering online.* **9**, 24 (2010).
45. Kawano, T. *et al.* Mechanical effects of the intraarticular administration of high molecular weight hyaluronic acid plus phospholipid on synovial joint lubrication and prevention of articular cartilage degeneration in experimental osteoarthritis. *Arthritis Rheum.* **48**(7), 1923–9 (2003).
46. Crisco, J. J., Blume, J., Teeple, E., Fleming, B. C. & Jay, G. D. Assuming exponential decay by incorporating viscous damping improves the prediction of the coefficient of friction in pendulum tests of whole articular joints. **221**(3), 325–33 (2007).
47. Liu, A., Jennings, L. M., Ingham, E. & Fisher, J. Tribology studies of the natural knee using an animal model in a new whole joint natural knee simulator. *J Biomech.* **48**(12), 3004–11 (2015).

Acknowledgements

This work is independent research funded by the National Institute for Health Research (Invention for Innovation (i4i), Development of manufacturing capability and pilot clinical evaluation of FibroFix: A mechanically advanced, tissue regenerative, meniscal cartilage repair device, II-LB-0417-20005). The views expressed in this publication are those of the author(s) and not necessarily those of the NHS, the National Institute for Health Research or the Department of Health and Social Care.

Author Contributions

D.W. carried out the experimental study as well as all analyses and drafted the manuscript. M.M. developed the test setup. L.d.R. and S.S. helped performing the experimental study and writing the manuscript. C.G., R.W. and N.S. supplied the scaffold material and proof read the manuscript. L.D. and D.W. conceived the study and L.D. and A.I. participated in its design and coordination. All authors read and approved the final manuscript.

Additional Information

Competing Interests: Authors Cristina Gentilini, Robert Walker and Nick Skaer are employees of Orthox Ltd. (Abingdon, UK). Oliver Kessler is a consultant to Orthox Ltd. (Abingdon, UK). All other authors declare no competing interest.

Publisher's note: Springer Nature remains neutral with regard to jurisdictional claims in published maps and institutional affiliations.



Open Access This article is licensed under a Creative Commons Attribution 4.0 International License, which permits use, sharing, adaptation, distribution and reproduction in any medium or format, as long as you give appropriate credit to the original author(s) and the source, provide a link to the Creative Commons license, and indicate if changes were made. The images or other third party material in this article are included in the article's Creative Commons license, unless indicated otherwise in a credit line to the material. If material is not included in the article's Creative Commons license and your intended use is not permitted by statutory regulation or exceeds the permitted use, you will need to obtain permission directly from the copyright holder. To view a copy of this license, visit <http://creativecommons.org/licenses/by/4.0/>.

© The Author(s) 2019